FULL SCALE RADIATION DOSE ANALYSES FOR THE SNS ACCELERATOR SYSTEM

Irina I.Popova and Franz X.Gallimeier
Oak Ridge National Laboratory, USA

Abstract

A radiation field appears in the SNS accelerator tunnel due to secondary particles created from the interaction of the proton beam halo with components along the proton beam line. During operations, the proton beam losses and secondary particles activate the structural materials and tunnel walls causing a residual radiation field of decay gammas after beam termination. Detailed dose rate analyses have been performed along the entire SNS accelerator line using MCNPX Monte Carlo code for the cases of operation, and after shutdown. A set of complex geometry models has been developed for the almost 900-m-long accelerator structure, and the losses along the proton beam line have been characterized with wide use of MCNPX geometry and general source cards capabilities. Dose rates due to residual radiation from the activated components were calculated in three steps using the Activation Analyses System in order to obtain residual gamma sources from activated components.

Introduction

The Spallation Neutron Source (SNS) [1] is powered by a high intensity, 2-mA, 1-GeV proton beam. Negatively charged hydrogen ions (H^-) are generated in an ion source and accelerated up to 1-GeV in a linear accelerator (linac) system, which is 325 m long and consists of a drift tube linac (DTL), a coupled cavity linac (CCL) and a superconducting linac (SCL) (Fig. 1). Then, the beam is transported through the 170-m-long high-energy beam transport (HEBT) line, which makes 90 degree turn, and is injected into an accumulator ring (248 m) by stripping away the electrons and starting out as a H^+ beam (proton beam). In the accumulator ring, the proton beam is accumulated through nominally one thousand turns, and then extracted from the ring and transported by the ring-to-target-beam transport (RTBT) line (150 m) to the mercury target station.

The H^- beam, which converts to the proton beam before injecting into ring, is not perfectly sized and develops a cloud of stray particles around itself, so called beam halo. The beam halo interacts with components along the accelerator and produces neutrons, gammas and other secondary particles in the accelerator tunnel - prompt radiation. The losses are the fractions of the beam particles, which are taken away from the beam due to interceptions and could be controlled and uncontrolled. During operations, the beam losses and secondary particles activate the structural materials and tunnel walls causing a residual radiation field of decay gammas after beam termination. Prediction of prompt and residual radiation fields in the accelerator tunnel is important to the project for the shielding designs optimizing and for the scheduling of maintenance personal access to the tunnel after beam termination.

Analyses were performed to study the impact of anticipated H^- and proton beam losses in the accelerator tunnel based on the beam loss characteristics, defined by the SNS beam loss document [2], both for the operation and maintenance periods. The MCNPX Monte Carlo code [3] was used as a tool for particles transport. The accelerator tunnel with beam forming and accelerating equipment is a long, almost 900-meters, and complex structure, which involves time-consuming input preparation, and particles tracking for the simulations. Both prompt and residual dose rates were calculated for the linac system and part of the accumulator ring. For the HEBT section, only the prompt radiation was estimated. Radiation analyses for the other sections of the accelerator system are in progress and will be presented in the future.

Geometry Model

Development of one large accelerator model is not feasible from the particles transport point of view because of computing limitations (hardware and software). Therefore, a set of four models: linac system, HEBT, accumulator ring and RTBT sections, was developed. Each model rigorously describes beam line components, and includes the accelerator tunnel environment including concrete walls and surrounding soil. The repeatable beam line components in each model were modeled using the MCNPX repeated structure capability, which allows us to describe each component in detail once, and then to place a rotated and shifted copy of the component multiple times at their locations.

Linear accelerator

The linac system model [4] describes the 325-m-long tunnel, which is 3-m high and 4.2-m wide, with 0.46-m thick ordinary concrete walls. The centerline of the beam is located 1.25-m above the floor and 1.75-m from one side wall. 5-m of soil surrounds the tunnel. The tunnel houses the DTL, the CCL and the SCL sections. The components forming each section differ significantly in shape, material and size (Fig. 2).

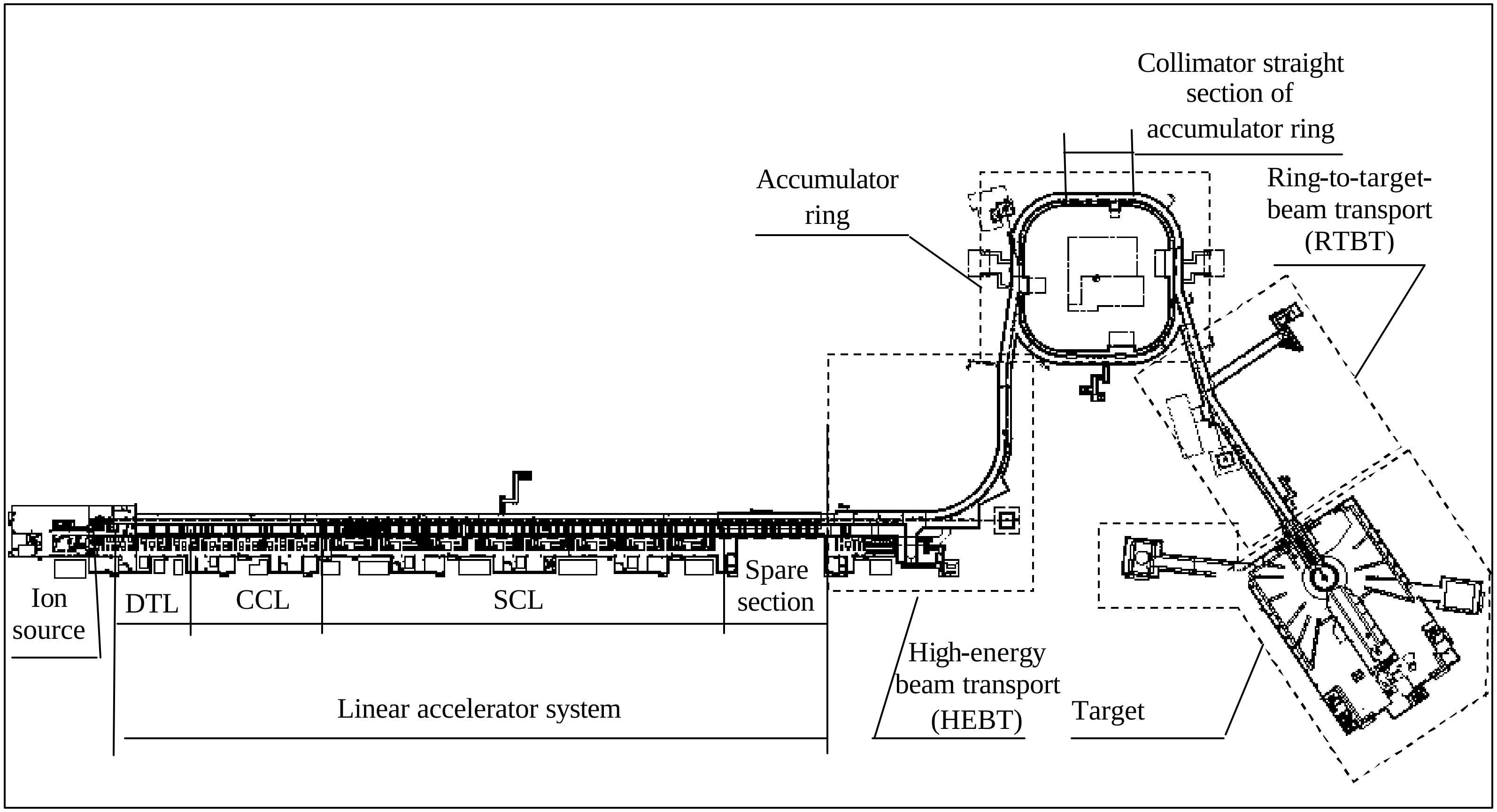

Figure 1. SNS Accelerator facility drawing.

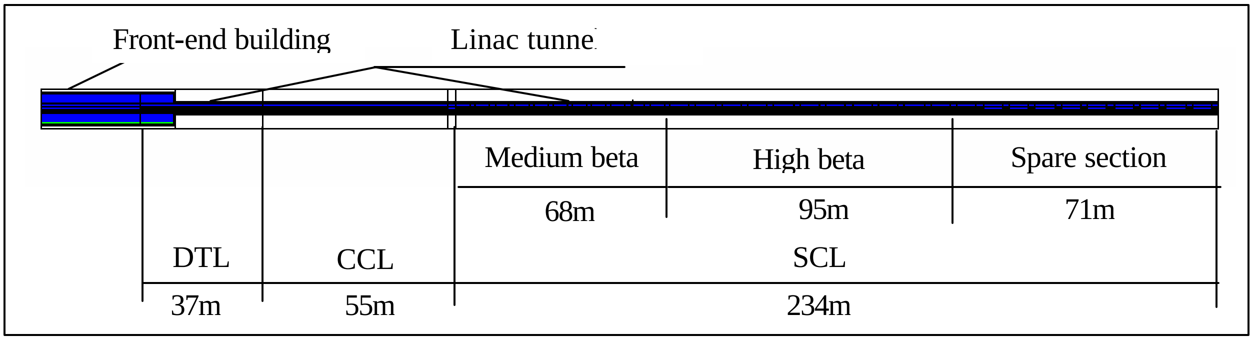

Figure 2. Linear accelerator system model for MCNPX analyses

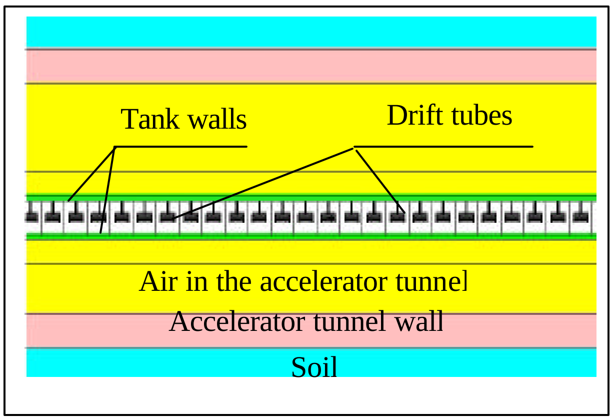

Figure. 3. Section of the MCNPX DTL model housing the drift tubes placed in a DTL tank.

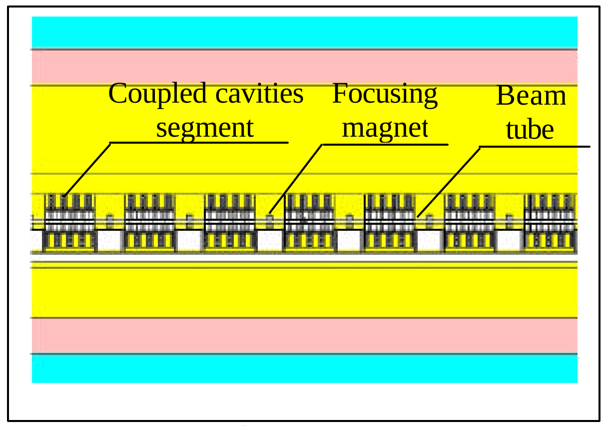

Figure 4. Section of the CCL model with complex cavity structure

The 37-m-long DTL section consists of 6 steel tanks (28-cm radius) with lined up drift tubes inside (Fig. 3).

The 55-m CCL section is a complex massive copper structure consisting of 4 modules. Each module has 12 coupled cavities segments, each of 76-cm of length, that are connected by a beam line and drums of powered coupler units. A focusing magnet is placed at the center of the connecting beam lines. Fig. 4 presents a sectional view of the model.

Compared to the CCL section, the SCL section is a very light structure relatively material mass. It consists of 11 medium beta cryomodules, and 12 high beta cryomodules. The total lengths of the medium beta and the high beta SCL are 68 and 95 meters, respectively. The SCL modules are connected with "warm" beam lines. A pair of magnets is placed at each of these beam line segments. The SCL modules are connected with "warm" beam lines. (Figs. 5 and 6). Each cryomodule was modeled as a voided cylindrical steel tank with a 98 cm inner diameter, 0.6 cm wall thickness closed at both ends with 1.0 cm thick plates. Each medium beta cryomodule houses 3, and each high beta cryomodule houses 4 aligned and inter-connected cylindrical helium filled steel vessels with 60 cm outer diameter and 0.2 cm wall thickness that themselves contain the bellows like super-conducting niobium cavities.

The SCL section extends with a 71-m long spare section that is intended to hold a future linac extension of 9 additional high beta SCL cryomodules that would produce H^- beam with energies up to 1.3

GeV. A period of this section consists of a steel beam pipe and a set of two steering magnets as shown in Fig. 7.

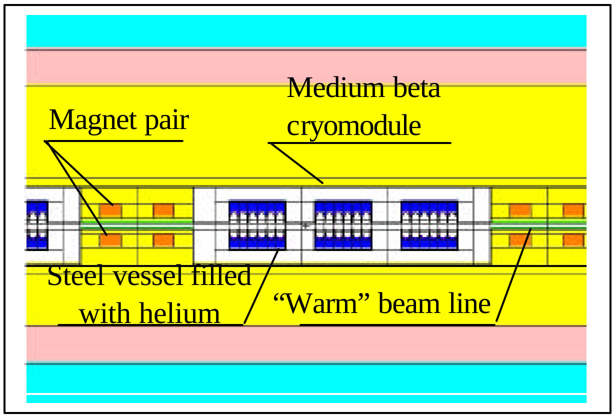

Figure. 5. Section of the MCNPX SCL model showing medium beta cryomoduls.

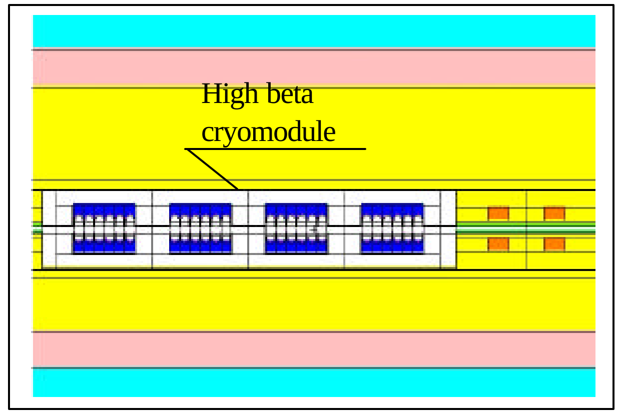

Figure 6. . Section of the MCNPX SCL model showing high beta cryomoduls.

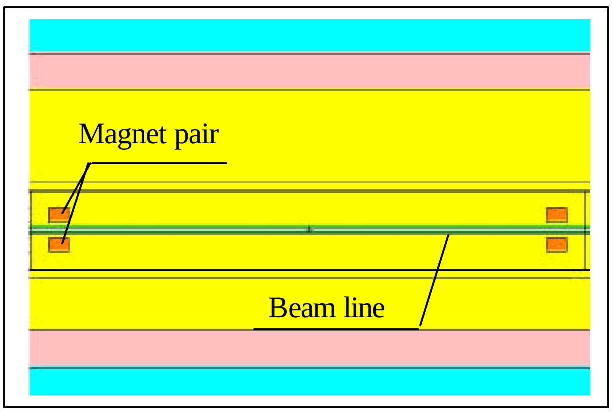

Figure 7. Section of the MCNPX SCL model showing spare section

As much use as possible was made of the lattice features of the MCNPX geometry capabilities to obtain a compact manageable geometry description culminating in a three-layer lattice hierarchy for the linear accelerator sections. For this reason the drift tube and cavity lengths that continuously increase with the H^- beam energy could not be easily modeled, which was a minor model disadvantage. Also vacuum pumps, supply lines, support structures, and other equipment in the accelerator tunnel, other than that mentioned above, were not considered.

HEBT

The HEBT model [5] describes a portion (129-meters) of the about 170-m-long tunnel that starts downstream of the long linear accelerator and exits into the accumulator ring. 75-cm-thick concrete walls form the HEBT tunnel, which is 4.3-m wide and 4.5-m high. The beam centerline is 1.25-m above the floor and 1.75-m from the tunnel wall. Various accelerator components are placed in the HEBT, accumulator ring and RTBT sections to collimate, correct and accumulate the beam. Figure 8 shows the MCNPX model for the HEBT. Blue, magenta and deep blue colors represent air in the accelerator tunnel, concrete walls and surrounding tunnel soil consequently.

The first 42 m of the HEBT tunnel is a long straight section housing 6 pairs of quadrupol magnets and correctors (quad/corrector pair), followed by a collimator, another quad/corrector pair, a second collimator, and 4 more pairs of quadrupoles and correctors. The 19-meters-long truck access tunnel is adjacent to the downstream end of the first straight section. The second 57-m section is curved over a 81.3-degree arc, with a beam line radius of about 36 meters. This curved section houses 8 large dipoles with a quad/corrector pair between each dipole and an arc beam stop. Only first 30-meteres from the third section are currently modeled. The section is straight and filled with 7 pairs of quadrupole magnets and correctors, and three traverse shield walls forming a maze.

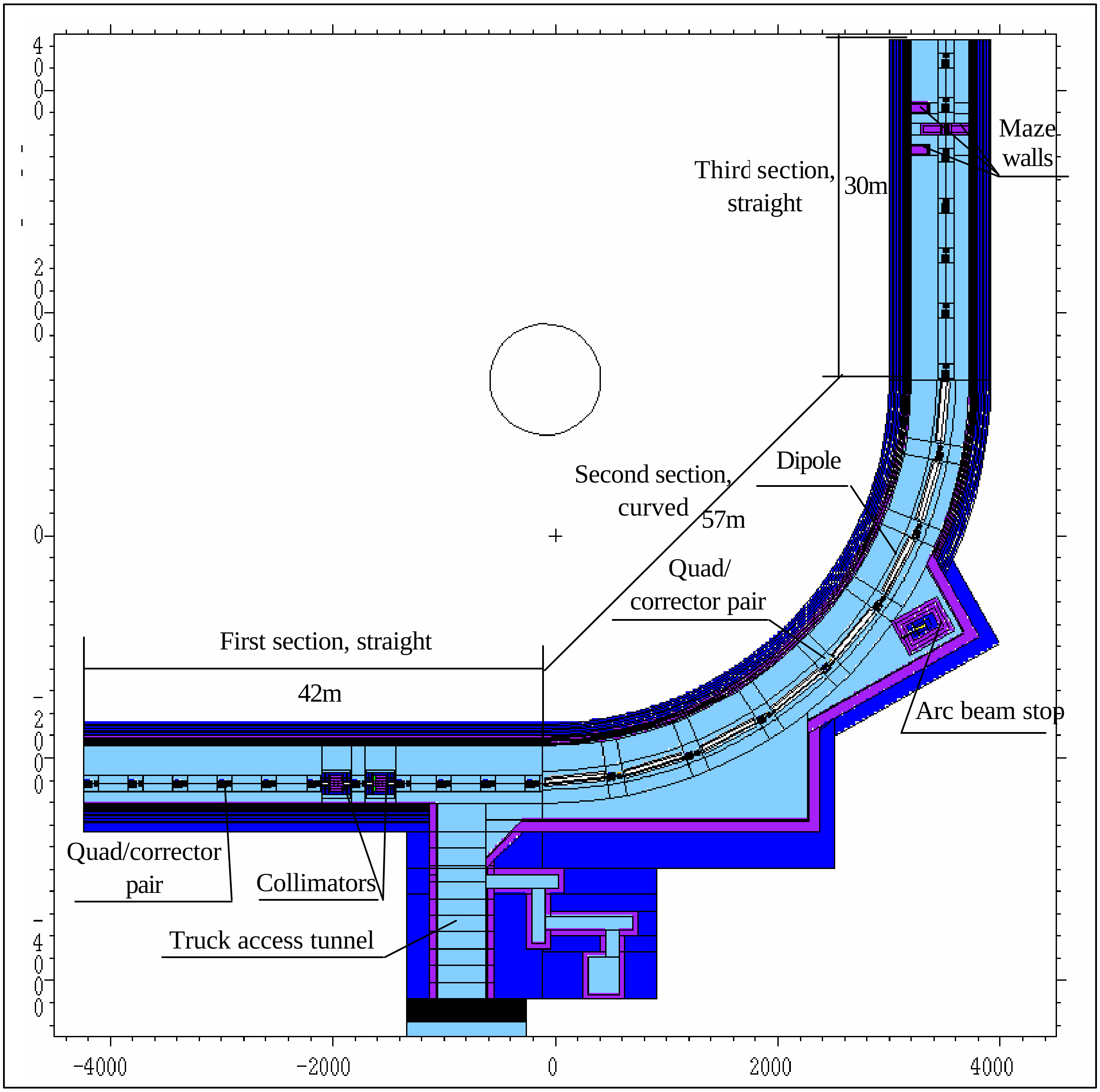

Figure 8.MCNPX model for HEBT

The large dipole magnets have an overall length of 5.7 m and are comprised of two sets of large horizontal copper windings with iron cores – one above and one below the beam line. The dipoles have a thick steel support structure on the top and bottom, which runs almost the full length of the dipole, as well as a thick back shielding plate facing the inner wall of the tunnel; the fourth side facing the outside wall of the tunnel is open. The quadrupoles each have 4 copper coils with individual iron cores, where the planes and the windings are normal to the beam, but where the coils themselves are physically rotated 45 degrees relative to the horizontal and vertical planes. The four coils are shielded and supported by thick external iron structure measuring 63-cm square on the outside and 77-cm in length. The corrector units downstream from the quadrupoles are smaller still and are about 41-cm square by 35-cm long. The collimators are more complex, heavily shielded, 1.8-m-diameter units with an overall length of 2.6 meters. The beam enters a large-diameter hole in the 66-cm-thick upstream iron shield, then passes through a thin platinum scraper. It enters a smaller diameter hole going through a 15-cm-long water-cooled section, and 1.2-meter-long particle bed, before emerging through the larger opening of the iron shield further downstream. The particle bed is 21.5 cm thick, with iron shielding extending beyond that to an outer radius of about 1 meter.

Each repeatable HEBT tunnel component has been modeled using the MCNPX repeated structure capability (transformation, universes and filling cards).

Accumulator ring

The accumulator ring consists from four straight sections that house the injection section, the collimation section, the extraction section and the bunching section. These sections are connected with 90 degree curved sections. Only the portion of the accumulator ring was modeled, where we expect the highest dose rate levels in the entire accelerator tunnel, because of the highest losses. A MCNPX geometry model [6] of components comprising the 30-meters-long collimator section, and the entering

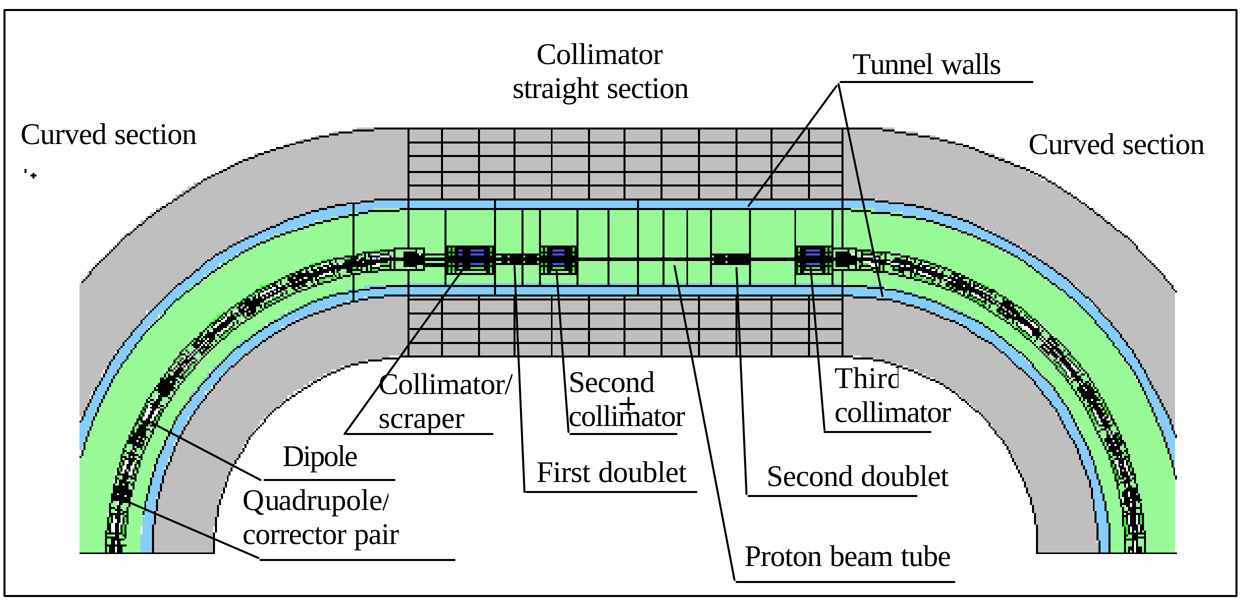

Figure 9. MCNPX model of accumulator ring portion, collimator straight section with two curved sections.

and exiting curved sections, which are 32-m long each, has been developed (Fig. 9). Grey and green colors represent the surrounding tunnel soil and air inside the tunnel respectively. The ring tunnel dimensions and wall thickness are the same as for the HEBT. 8 dipoles and 9 quadrapole/corrector pairs as described above are lined up by turns in each curved beam line section. These components have been modeled using the MCNPX repeated structure capability. All components in the straight collimator line are modeled directly and consecutively along the proton beam. This part of the tunnel contains one scraper/collimator, a doublet, a second collimator, a second doublet and a third collimator. Each doublet consists of a corrector and two quadrupoles. The collimators are similar to the HEBT collimators.

Sources

The sources for the transport calculation during the operation are the beam (H^- or proton) losses and defined as a fraction of the beam, interacting with the beam tube and equipment. The losses are not uniformly distributed in each accelerator section and the lost fraction of the beam depends on the location. For the linac system, where beam accelerates from 65 KeV to 1 GeV the source is even more complex - the radii from the beam center line to the place of interaction (aperture), the angle of interaction relatively to beam direction, and energy are changing along the accelerating line (Fig 10). The sources were modeled with the standard MCNPX input cards using extensively the conditional probability distributions.

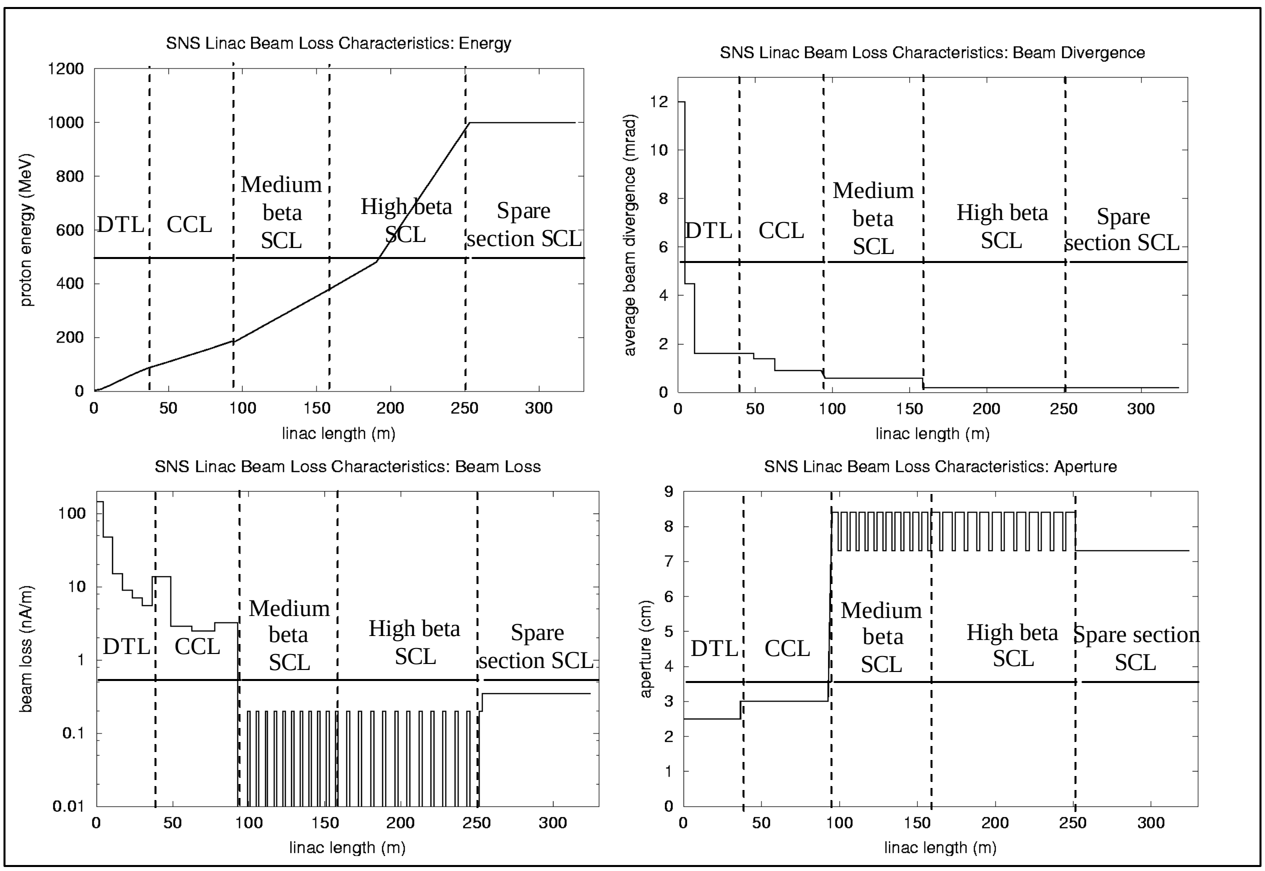

Fig. 10: Characteristics of the anticipated proton beam losses in the SNS linac system during normal operation [2]

Only uncontrolled losses appear in the linear accelerator system. Eight source points were defined around the circumference of the beam aperture at 450 locations along the linac length with energy, position, and flight direction adjusted to the definitions.

In the HEBT section, accumulator ring section and RTBT section uncontrolled losses are 1 watt/m, which could appear everywhere and correspond to the $5*10^{-7}$ beam fraction/m. Figure 11 shows the fractional controlled losses in the straight collimator section of the ring. The controlled losses appeared as well in both HEBT collimators ($5*10^{-6}$ in each), in the HEBT arc beam stop (10^{-3}) and in the RTBT collimators.

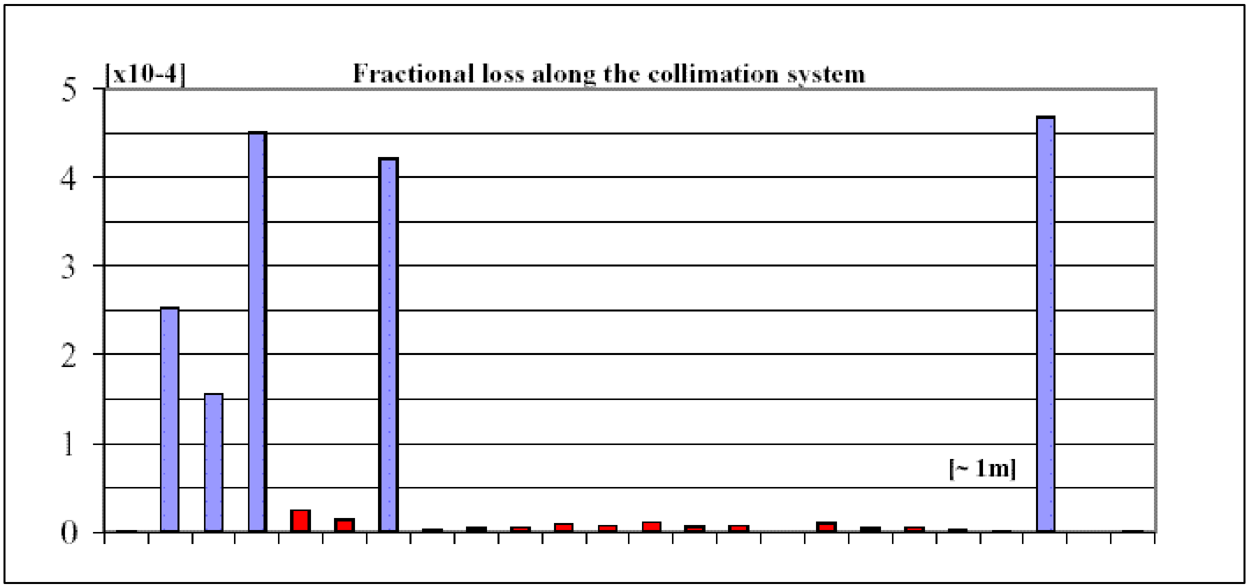

Figure 11. Loss distribution along the accumulator ring collimator straight section. The data are fractional loss assuming a total loss $1.9\cdot10^{-3}$ from the full beam.

The proton beam losses were described as a continuous set of cylindrical surface sources with 9.1-cm radius for the accumulator ring section and a 2.6-cm radius for HEBT section located inside the beam tube, with uniformly distributed 1 GeV protons along each cylindrical surface. The direction of the protons, as the direction of axis of each cylinder, is parallel to the direction of the nominal proton beam. The source intensity in each cylindrical surface source corresponds to the integral beam losses in the specified component.

Methods

The dose rates at 30-cm distance from the beam line components were estimated performing transport calculations with the MCNPX Monte Carlo multi-particle transport code running in a parallel computer environment using PVM mode. Surface flux tallies, combined with the energy-dependent flux-to-dose conversion coefficients from the HILO multi group cross section library [7] with 83-neutron and 22 gamma groups, have been applied to obtain neutron and gamma doses.

The residual dose rates analyses are complex for the high energy transport calculations and involve different codes and data libraries. The analyses of dose rate due to residual activation of materials in the accelerator have been performed in three steps. In the first step, the neutron fluxes below 20 MeV and isotope production rates induced by above 20MeV particles were calculated in each cell of the sections' components using the Monte Carlo code MCNPX. The geometry model used for the prompt radiation calculations has been slightly modified. Some thick cells were subdivided into a few thinner cells to obtain a more detailed activation profile. The repeated structures were converted into regular ones, because code could not resolve activation of the repeated cells. The linear accelerator detailed model was converted into simplified model of accelerator components mostly in cylindrical geometry, where the spare sections were homogenized into larger cells.

For the second step, the Activation Analyses System (AAS) [8], which is a set of scripts built around the ORIHET95 isotope production and depletion module [9], has been used. This system reads neutron fluxes below 20 MeV from the MCNPX calculation and folds them with the FENDL-based isotope production cross sections for each nuclide in each material. Then the low-energy nuclide production rates are combined with the high-energy production rates from MCNPX calculation to obtain the total production rates for all resulting nuclides in each cell. These total production rates are then fed into the ORIHET code. The ORIHET code uses the total production rates, as well as a decay library, for the final buildup/decay calculations. ORIHET95 produces isotope concentration and activation tables, and tables of gamma spectra and gamma power in the multi-group structure of the DABL69 and HILO libraries.

In the third step the gamma production spectra and gamma power were extracted from ORIHET outputs for each cell and formatted into source descriptions in the MCNPX input language using a specially created interface program. MCNPX picks the cell from a probability table reflecting the photon source strengths, and samples the energy from the gamma spectra. The source location within the cell is randomly sampled with the rejection techniques. The MCNPX input allows 999 distribution functions to be used for a source distribution. This limits the number of cells with activation sources to be applied in one calculation. For one cell the user has to specify the energy distribution, and radial and axial spatial distributions to be used for sampling the source location with the rejection technique. At least three distribution functions per cell are required, meaning that about 300 activation cells can be included into the source. The number of cells in the model for each section exceeded this limit. Consequently, the activation calculations had to be performed in pieces. The linear accelerator section was subdivided into 3 models: DTL, CCL and SCL. The residual analyses for accumulator ring were performed only for the collimator straight section. Furthermore, for each sub-model two calculations were performed: with residual gamma sources located in the components along the beam line, and with residual gamma sources located in the tunnel walls. Nevertheless, the separate calculations give the advantage of determining the influence of both residual sources: equipment and concrete walls, into the integrated residual dose rate.

Residual dose rate were analyzed for one hour decay period following 30 years continuous operation.

Results

The prompt doses at 30-cm distance from the equipment in the linac are shown in Figure 12. The dose-rates level rises in the beginning of the linac, in the DTL section, with increasing beam energy to the 10 rem/hr level, and peaks with 80 rem/hr and 60 rem/hr at the start and the end of the CCL section, reflecting local peaks in the beam losses. In the SCL, the dose-rates level drops down due to lower beam losses and rises slightly with beam energy increasing. The beam losses increase significantly in the SCL spare section and cause peak values of 200-rem/hr due to higher beam losses caused by higher vacuum.

Residual dose levels of up to 5 mrem/hr were found in the DTL, 20-30 mrem/hr in the CCL, 2-5 mrem/hr in the SCL, and up to 40 mrem/hr in the spare section as demonstrated in Figs. 13 through 15. Thus the residual dose rates in the linear accelerator tunnel are a factor of 2000-3000 lower than the operational dose rates.

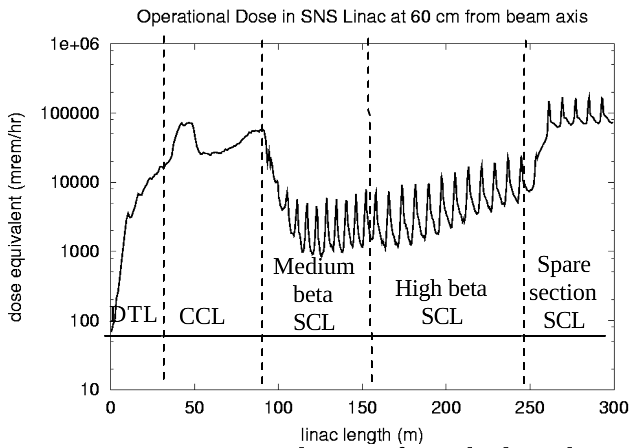

Fig. 12: Dose at 60 cm distance from the linac beam axis due to beam losses in normal operation

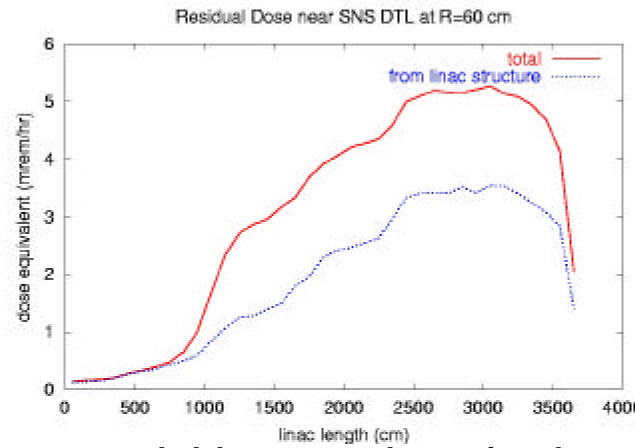

Fig. 13: Residual dose at 60 cm distance from the beam in the DTL after 30 years of operation and 1 hour after shutdown.

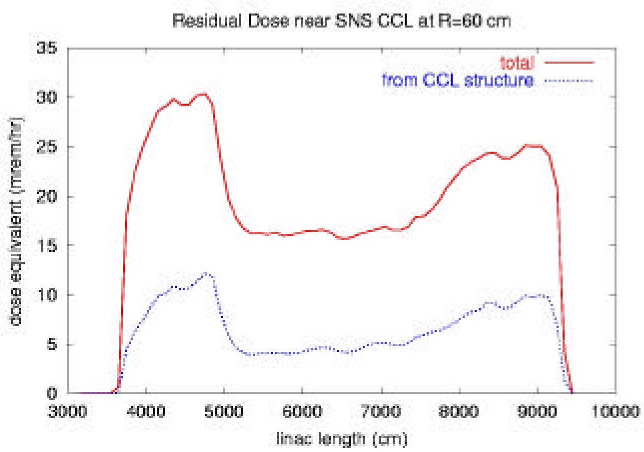

Fig. 14: Residual dose at 60 cm distance from the beam in the CCL after 30 years of operation and 1 hour after shutdown

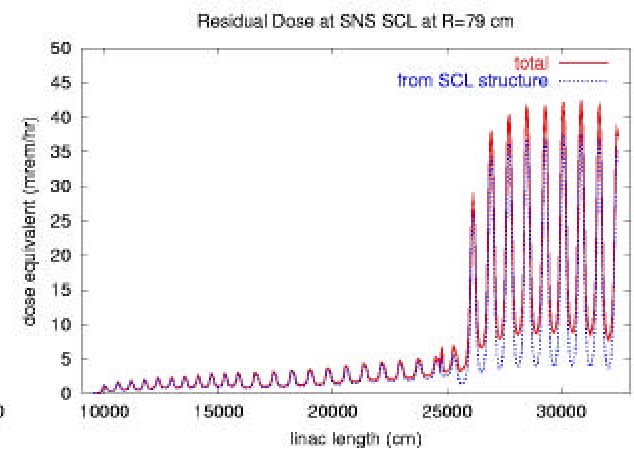

Fig. 15: Residual dose at 60 cm distance from the beam in the SCL after 30 years of operation and 1 hour after shutdown

The prompt dose rate levels in the HEBT vary from 117 rem/h to 500 rem/h (Fig. 16). The collimator locations are marked by the gray shaded areas. Although the highest proton losses in the HEBT along the beam line are located in both collimators, there is a decrease of the dose rate levels in their locations due to effective collimators' shielding in the radial directions. The first dose rate peak corresponds to the location of the first dipole, first component in the curved section, because this component has a U shape and does not provide any shielding in the direction from the beam line to the tunnel wall. Around the next components there is a dose rate decrease due to curved shape of the beam direction, plus the front structures of the components provide the shielding. In the fourth down stream dipole (Fig. 8) there is a second peak due to the radiation back scattering from the arc collimator.

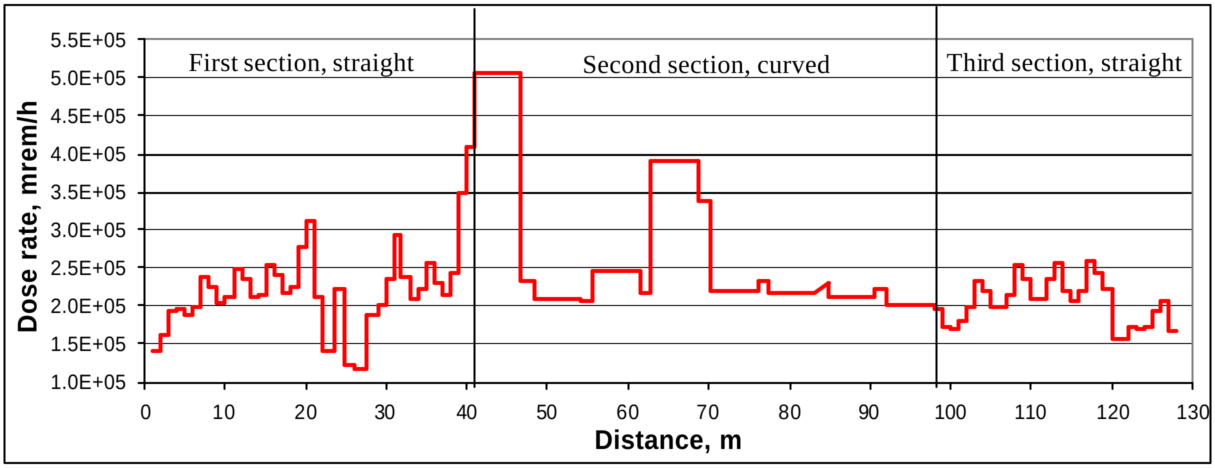

Figure 16. Prompt neutron dose rates in the HEBT

The collimator straight section of the accumulator ring has the highest losses along the proton beam line in the SNS accelerator line and consequently the highest dose rate. Figure 17 shows prompt dose rates distribution in this area. The red line describes the neutron doses; the blue line describes the gamma doses. The collimator locations are marked by the gray shaded areas. Although the highest proton losses are located in the collimators, the highest dose rates show up in the areas downstream of the collimators. The collimators are heavily shielded but more effectively in the radial direction than in the axial direction. Hence, there is a high probability of protons and secondary particles leaking out through the beam tube opening since the particle distributions are forward directed and create a higher radiation fields in less shielded areas.

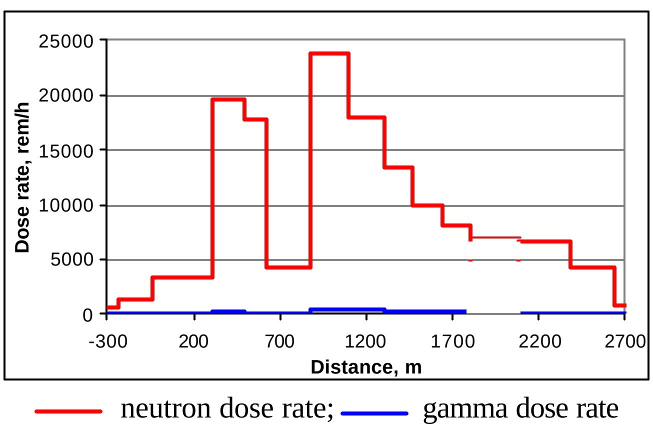

Figure 17. Prompt dose rates in the collimator straight section at 30-cm distance from the beam line components

The residual dose distribution along the beam shows a profile similar to the operational dose rate profile in the sense that there is an increase of the dose levels directly after the collimators. Figure 18 shows the residual dose distribution from both the concrete wall and the equipment after 30-years of operation and one hour of cool down. The area with the highest dose is located around the beam tube downstream the second collimator.

Analysis shows that the residual doses in the collimator section tunnel of the ring are a factor of 1000-1700 lower than the operational doses.

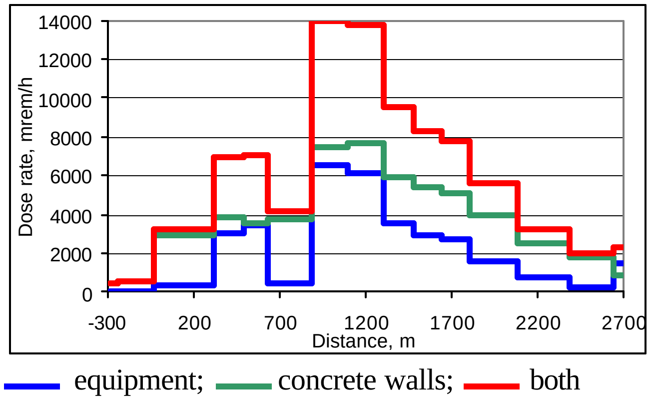

Figure 18. Residual dose rate distribution in the collimator straight section after 30 years operation and one hour cool down at 30-cm distance from the beam line components

Conclusions

A full scale set of complex and large MCNPX models of SNS accelerator system including linear accelerator, HEBT and accumulator ring was developed for the analyses of prompt and residual dose rate in the accelerator tunnel environment. Each model rigorously describes the beam line components housed in the accelerator tunnel with wide use of MCNPX repeated structure capabilities, both lattice and transformation. The prompt and residual dose rates were estimated with acceptable statistics (below 10%) and were applied for finding shielding solutions, whenever it was necessary, and for the scheduling of maintenance personal access to the tunnel after the beam termination.

Peak doses of 25000rem/h were predicted in the accumulator ring collimator straight section during normal operation, which will result in peak residual doses of 14 rem/h. Therefore this area will be closed off for the access by the mesh fences. All other tunnel sections, so far investigated, are radiations areas with restricted access.

The calculation full scale set of modules developed for the SNS accelerator is currently being used for other applications such as activation analyses, sources for radiation transport through the penetrations in the accelerator tunnel, dose levels on the top of the soil on the accelerator and so on.

References

[1] National Spallation Neutron Source Conceptual Design Report, Oak Ridge National Laboratory, NSNS/CDR-2/VI, 1997.

[2] N. Catlan-Lasheras et. al., "Accelerator physics model of expected beam losses along the SNS accelerator facility during normal operation," ANA/AP Technical Note 07, UT-Battelle, LLC, Oak Ridge (March, 2001).

[3] L.S. Waters, ed., *"MCNPX User's Manual – Version 2.1.5"*, Los Alamos National Laboratory, NM, TPO-E83-G-UG-X-00001, Nov. 1999.

[4] F. X. Gallmeier, "Calculations of Operational and Residual Doses for the SNS Linac"

[5] J. A. Buchholz, “Determination of Proton, Neutron, and Gamma Boundary Source Terms for Subsequent Egress Shielding Analyses in the SNS HEBT Tunnel”, UT-Battelle, ORNL/SNS-106100200-TR0017-R00, September 2000.

[6] I. I. Popova and J. A. Bucholz, “Neutron and Gamma Source Terms around the Egress Adjacent to the SNS Accumulator Ring”, UT-Battelle, ORNL/SNS-106100200-TR0020, September 2000.

[7] R. G. Alsmiller jr., J. M. Barnes, and J. D. Drischler, *Neutron-Photon Multigroup Cross Sections for Neutron Energies Less than or equal 400 MeV (Revision 1)*, Oak Ridge National Laboratory, ORNL-TM 9801 (February 1986).

[8] Greg McNeilly, *“AAS-Activation Analysis System”*, SNS-101040200-TR0003R00, UT-Battelle (1999).

[9] F. Atchison, “*OriHet95 for the VAX*”, ORNL, internal documentation, 1984